Rocky Worlds DDT: JWST/MIRI Scheduling Report for LHS 1140 b

Munazza K. Alam, Tyler Baines, Rachel A. Cooper | ***JWST Target Scheduling Team***
Néstor Espinoza, Hannah Diamond-Lowe | ***RWDDT CIT Leads***

The Rocky Worlds Director's Discretionary Time (RWDDT) program will observe 9 eclipses of the rocky exoplanet LHS 1140 b using MIRI Imaging photometry with the F1500W filter. As detailed below, the JWST Target Scheduling Team has refined the orbital parameters (§1) for this planet and has used these values to calculate the phase constraints and observation windows (§2), as well as the APT inputs (§3).

1 ORBITAL PARAMETER CALCULATIONS

The nearby M-dwarf system LHS 1140 hosts two confirmed transiting exoplanets. The RWDDT target LHS 1140 b is a $1.73R_{\oplus}$, $5.60M_{\oplus}$ exoplanet orbiting on a 24.7-day period orbit — in the habitable zone of its star (Dittmann et al., 2017; Cadieux et al., 2024a). Its sibling, LHS 1140 c, is a $1.27R_{\oplus}$, $1.91M_{\oplus}$ exoplanet orbiting in a shorter, $3.7 - day$ period orbit around the host star (Ment et al., 2019). R. Cooper performed joint orbital fitting of available ground- and space-based data to update the eclipse ephemerides for scheduling the RWDDT observations.

1.1 AVAILABLE DATA

Photometric and radial velocity (RV) data used for the orbital fitting described in Cadieux et al. (2024b) were shared by C. Cadieux, in addition to extracted photometry from the two NIRISS SOSS transits obtained as part of JWST DD 6543 (PIs: Cadieux & Doyon) and analyzed in Cadieux et al. (2024a). These data were already corrected for various systematics, so no additional detrending was performed prior to fitting. For a complete description of the data reduction procedure for each instrument, see the above cited papers. Additionally, M. Fortune shared three MIRI 15 μm eclipse observations of LHS 1140 c from Fortune et al. (2025), which were also incorporated into the joint fits. These observations were obtained as part of the Hot Rocks Survey (GO 3730; PIs: Diamond-Lowe & Mendonça).

The time series and RV data used in our global orbital parameter fits are summarized below:

- Photometry: TESS[1] Sectors: 3 & 30; Spitzer; HST/WFC3; JWST/NIRISS SOSS; JWST/MIRI F1500W
- Radial velocity: ESPRESSO, HARPS

1.2 RESULTS

Initial fits were performed using the same Bayesian priors as those in Cadieux et al. (2024b), and resulted in nearly identical median posteriors for the orbital parameters

[1]Retrieved from the MAST Archive

Parameter	juliet$_{circ}$	juliet$_{ecc}$
P [days]	$24.73725^{+1.374\times10^{-6}}_{-1.292\times10^{-6}}$	$24.73725^{+1.203\times10^{-6}}_{-1.141\times10^{-6}}$
t_0 [BJD$_{\rm TDB}$]	$2458399.93033^{+9.82415\times10^{-5}}_{-1.04871\times10^{-4}}$	$2458399.93035^{+8.74479\times10^{-5}}_{-9.13385\times10^{-5}}$
ω [deg]	-	$33.06^{+62.69}_{-54.56}$
e	-	$0.017^{+0.017}_{-0.012}$
b	$0.142^{+0.033}_{-0.039}$	$0.138^{+0.036}_{-0.050}$

Table 1: Posterior estimates of the orbital parameters for LHS 1140 b assuming circular and eccentric orbits from our `juliet` fits. The reported uncertainties correspond to 1σ Bayesian credible intervals.

of interest. We then also included the HARPS RV data omitted from Cadieux et al. (2024b), the NIRISS/SOSS transits of LHS 1140 b , and the MIRI eclipses of LHS 1140 c, and ran global fits allowing for either a circular or eccentric orbit for LHS 1140 b . We utilized the `juliet` package's capability to jointly fit transit, eclipse, and radial velocity data for multiple planets simultaneously (Espinoza et al., 2019). Most priors were adopted directly from Cadieux et al. (2024b). For the MIRI data, however, we included an additional linear + exponential detrending model due to strong instrumental systematics at the beginning of the time series. We also fit a GP to each photometric dataset with a `celerite` approximate Matérn kernel, and to the radial velocity data with a quasi-periodic kernel. The orbital parameters obtained from those fits and required for scheduling the RWDDT MIRI F1500W observations of LHS 1140 b 's secondary eclipses are presented in Table 1.

The difference between the mid-eclipse times for the eccentric and circular cases is $\sim$2.9 hours for an eclipse occurring in December 2025. The 1σ uncertainty of the eclipse timing is $^{+6.7929}_{-3.7248}$ hours for the eccentric solution and $^{+0.0011}_{-0.0010}$ hours for the circular solution. The difference in log Bayesian evidence suggests very weak evidence in favor of the circular orbit ($\Delta \ln Z < 3$).

2 OBSERVING STRATEGY

To determine the number of eclipses needed for this target, N. Espinoza and H. Diamond-Lowe followed the RWDDT 2-checkpoint strategy[2] and calculated that 9 eclipse observations of LHS 1140 b are required to differentiate a 1 bar CO_2-dominated atmosphere case from a zero-albedo bare rock case at 3σ with a statistical power of 80% (assuming JWST ETC MIRI/F1500W noise $\times 1.25$, enhanced to account for systematic and/or astrophysical noise).

T. Baines then followed the Tinker Scheduling strategy used in prior RWDDT observations (e.g., DD 9235) to calculate the observing windows and phase constraints for each of the 9 eclipses (Figure 1). The minimum and maximum phase, zero phase, total time on-target, and number of integrations per eclipse observation are reported

[2]RWDDT 2-checkpoint strategy: `https://rockyworlds.stsci.edu/rw-website-schedule.html#strategy`

in Table 2.

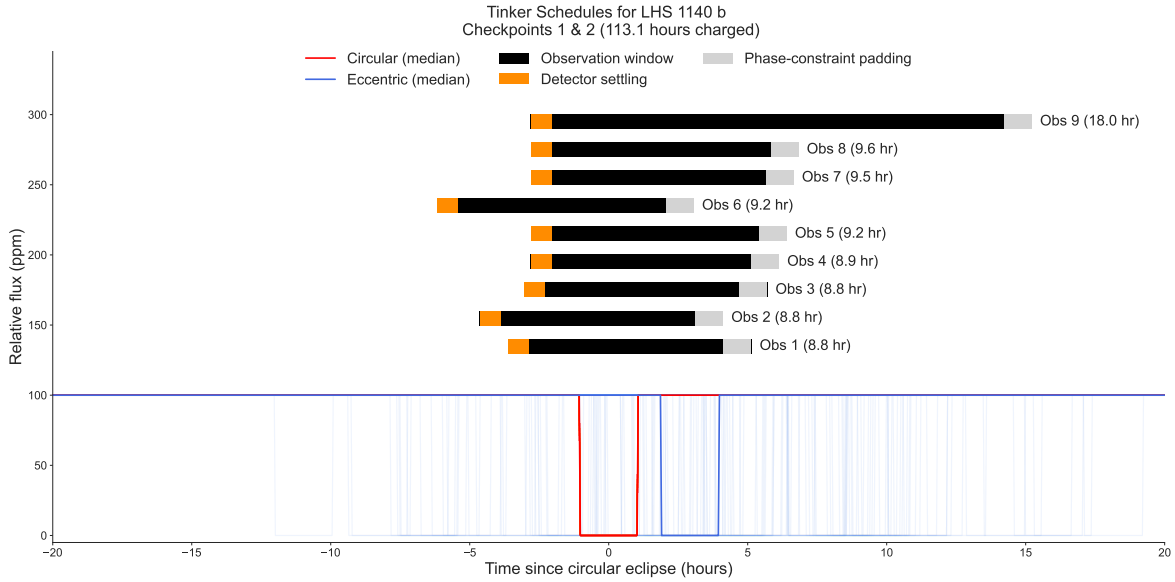

Figure 1: Observation windows for MIRI 15 μm secondary eclipses of LHS 1140 b, based on the 2-checkpoint and Tinker Scheduling strategies.

3 APT INPUT CALCULATIONS

Calculations for the APT file and the ETC were performed by T. Baines and M. Alam. Using system parameters from the NASA Exoplanet Archive, we updated the mid-eclipse time, orbital period, impact parameter, and eccentricity to the best-fit values from R. Cooper's circular `juliet` fits. We then calculated the optimal configuration for these MIRI Imaging time-series observations using the F1500W filter. All instrumental parameters assume a 65% saturation limit to preserve detector linearity while maximizing SNR. The selected configuration (calculated with APT 2025.1, JWST ETC 4.1, Pandeia 4.0) uses the SUB256 subarray with FASTR1 readout and 47 groups per integration (Table 3). We also retrieved the updated right ascension (RA), declination (Dec), parallax, proper motion RA, and proper motion Dec from Gaia Data Release 3 (Gaia Collaboration et al., 2016, 2023), as shown in Table 3.

M. Alam also performed ETC calculations (Workbook ID 287295) using a PHOENIX M5V stellar model ($T_{\rm eff} = 3500$ K, $\log g = 5.0$) normalized to $K = 8.8$ mag. For the observing setup in the ETC, we specified the SUB256 subarray, FASTR1 readout mode, and 47 groups per integration. Since the total time on target varies for each of the 9 eclipse observations in the 2-checkpoint strategy, the number of integrations per exposure is shown in Table 2 for each observation.

Our observational setup yields no errors or warnings in the ETC or in APT. Observations 8-9 were placed on hold to decide on possible changes to the phase constraints after Observation 7. To enforce the tinker scheduling order of eclipses (i.e., from shortest to longest observing window), we included BETWEEN windows in the Special Requirements section of the APT. These windows also ensure that we do not schedule our observations during overlapping transits or eclipses of the sibling planet LHS 1140 c.

Table 2: Comprehensive Observation Planning Parameters for LHS 1140 b

(c) Eclipse Observation Schedule

Phase constraints and exposure parameters from Tinker Scheduling analysis

Obs	$\phi_{\min}$	$\phi_{\max}$	t_0 (HJD)	t_{total} (hr)	n_{ints}
1	0.9909463	0.9926309	2461034.478	8.75	2192
2	0.9909463	0.9926309	2461034.478	8.75	2192
3	0.9909463	0.9926309	2461034.436	8.75	2192
4	0.9907963	0.9924809	2461034.516	8.93	2236
5	0.9905613	0.9922459	2461034.522	9.21	2306
6	0.9905541	0.9922387	2461034.382	9.22	2308
7	0.9903503	0.9920348	2461034.527	9.46	2369
8	0.9902038	0.9918884	2461034.531	9.63	2412
9	0.9831365	0.9848211	2461034.706	18.03	4514

Table 3: APT input parameters for LHS 1140 b

APT Input Parameters

Based on `juliet` circular orbital solution (APT 2025.1, JWST ETC 4.1, Pandeia 4.0)

(b) MIRI Instrument Configuration

Parameter	**Value**	**Unit**
Detector Subarray	SUB256	—
Number of Groups	47	—
Detector Settling Time	0.75	hr
Pre-eclipse Baseline	1.0	hr
Post-eclipse Baseline	1.0	hr
Eclipse Duration	2.1	hr

(c) Target Astrometric Parameters

Parameter	**Value**	**Unit**
Right Ascension (J2016.0)	00:44:59.683	h:m:s
Declination (J2016.0)	-15:16:27.089	d:m:s
Parallax	66.829	mas
Proper Motion (RA)	318.152	mas yr^{-1}
Proper Motion (Dec)	-596.623	mas yr^{-1}

References

Cadieux, C., Doyon, R., MacDonald, R. J., et al. 2024a, , 970, L2, doi: 10.3847/2041-8213/ad5afa

Cadieux, C., Plotnykov, M., Doyon, R., et al. 2024b, , 960, L3, doi: 10.3847/2041-8213/ad1691

Dittmann, J. A., Irwin, J. M., Charbonneau, D., et al. 2017, , 544, 333, doi: 10.1038/nature22055

Espinoza, N., Kossakowski, D., & Brahm, R. 2019, , 490, 2262, doi: 10.1093/mnras/stz2688

Fortune, M., Gibson, N. P., Diamond-Lowe, H., et al. 2025, arXiv e-prints, arXiv:2505.22186, doi: 10.48550/arXiv.2505.22186

Gaia Collaboration, Prusti, T., de Bruijne, J. H. J., et al. 2016, , 595, A1, doi: 10.1051/0004-6361/201629272

Gaia Collaboration, Vallenari, A., Brown, A. G. A., et al. 2023, , 674, A1, doi: 10.1051/0004-6361/202243940

Ment, K., Dittmann, J. A., Astudillo-Defru, N., et al. 2019, , 157, 32, doi: 10.3847/1538-3881/aaf1b1